Domain Decomposition Methods for Multiscale Modeling

105

Xin Bian and Matej Praprotnik

Contents

Abstract

Domain decomposition methods (DDM), which originate from the Schwarz alternating method to solve elliptic partial different equations, are largely extended and prove to have increasing influences on multiscale modeling of materials. We discuss some of the important extensions of the DDM in the fields

X. Bian (✉)
Computational Science and Engineering Laboratory, Clausiusstrasse, ETH Zurich, Switzerland
e-mail: bianx@ethz.ch

M. Praprotnik
Laboratory for Molecular Modeling, National Institute of Chemistry, Ljubljana, Slovenia

Department of Physics, Faculty of Mathematics and Physics, University of Ljubljana, Ljubljana, Slovenia
e-mail: praprot@cmm.ki.si

W. Andreoni, S. Yip (eds.), *Handbook of Materials Modeling*,
https://doi.org/10.1007/978-3-319-44680-6_65

of multiscale modeling for soft materials such as simple and complex fluids. To this end, we typically model the fluids in two or more levels of detail, which exploits the computational efficiency of the coarse model and physical accuracy of the fine description. For simple fluids, we take a continuum perspective to couple the molecular dynamics (MD) and Navier-Stokes equations by matching the state variables and/or fluxes across the hybrid interface. For complex fluids, we take a discrete perspective to encompass the complex structure of the molecules and couple the MD with coarse-grained MD by interpolating the forces between the two levels of descriptions.

1 Introduction

Domain decomposition methods (DDM) may represent a generic concept of solving a problem defined on a global domain by first dividing the domain into a set of overlapping/non-overlapping subdomains. Given that the set of the subdomains covers the original domain and a local problem is solved in each subdomain, the solution for the original global problem is available. Therefore, in a nutshell, it is a methodology of "divide and conquer." However, such a generic concept may be interpreted quite differently in various disciplines.

The name of DDM is mostly referred in applied mathematics, where it represents the decomposition of partial differential equation (PDE) or its approximation on the whole domain into a set of coupled problems on interconnecting subdomains. This dates back to the classical Schwarz alternating method proposed in 1870 (Smith et al. 1996), where the solution of an elliptic boundary value problem is obtained by alternatively solving two same elliptic boundary value problems defined in the two overlapping subdomains. For a general classification of DDM, the decomposition of domain may enter (Toselli and Widlund 2005):

1. At the continuum level, where different PDE models are appropriate for different regions. For example, in the applications of fluid-structure interactions, the fluid and solid regions are described by PDEs of fluid and solid mechanics, respectively. Another example is the aerodynamic boundary layer proposed by Ludwig Prandtl in 1904 (Landau and Lifshitz 1987); in the vicinity of bounding surface, viscous effects of the fluid are significant, while far away from the surface, a description of inviscid flow is sufficient.
2. At the discretization level, where different approximation schemes are employed in different regions. For example, a finite difference method is adopted in one region, while a finite element method is preferred in the other region.
3. At the algebraic level, where a large linear (sparse) system of equations results from the discretization of the PDE. A global iterative method may be inefficient so that a strategy from DDM may choose to solve each block of the linear system individually by employing a direct or iterative method. In this context, the DDM is considered as a preconditioner in combination with other acceleration

techniques such as Krylov space methods. The numerical analysis of DDM as a preconditioner is very developed, which may be found in excellent monographs (Smith et al. 1996; Quarteroni and Valli 1999; Toselli and Widlund 2005).

In practice of numerical modeling, the decomposition at these three levels mentioned above may be interconnected.

Utilizing the idea of DDM for multiscale modeling with heterogeneous mathematical/physical descriptions is also not a new concept. In computational chemistry, one of the earliest examples is the QM/MM (quantum mechanics/molecular mechanics) (Warshel and Karplus 1972; Warshel and Levitt 1976), where chemical reactions involving large molecules are handled by quantum mechanics and regions at elsewhere by classical models. Typically, the degrees of freedom for the two descriptions are fixed during the course of the simulation.

A sudden increase of attention in applying DDM for multiscale modeling of fluids started with the paper of O'Connell and Thompson (1995), where one subdomain is simulated by molecular dynamics (MD) with Lennard-Jones potential, while the other subdomain is solved by a finite difference method discretization of the Navier-Stokes (NS) equations. The overlapping region of the two subdomains implements the "handshaking" of the physical models at two scales. Since the inception of this work, many further important contributions emerge, especially on the constraint dynamics of MD's artificial boundary such as the Maxwell buffer (Hadjiconstantinou and Patera 1997; Hadjiconstantinou 1999), flux-exchange method (Flekkøy et al. 2000; Delgado-Buscalioni and Coveney 2003a; Flekkøy et al. 2005; De Fabritiis et al. 2006), least constraint dynamics (Nie et al. 2004; Werder et al. 2005), adaptive forcing (Pivkin and Karniadakis 2006; Fedosov and Karniadakis 2009), and so on. These methodologies are from a continuum perspective of fluid mechanics, and the coupling of two distinct scales is mainly for modeling simple liquids. There exist a few excellent review articles on this topic (Wijesinghe and Hadjiconstantinou 2004; Mohamed and Mohamad 2010; Delgado-Buscalioni 2012).

Another important research line on DDM for multiscale modeling of structured or complex fluids is represented by the adaptive resolution scheme or AdResS from computational physics/chemistry. In one subdomain, a detailed MD model with atomic details is employed, while in the other subdomain, a coarse-grained (CG) model is adopted. The CG model is usually constructed off-line and, if required, is able to reproduce quantities of interest from MD faithfully. A complex molecule may diffuse across the interface between the two subdomains and change degrees of freedom gradually. In the overlapping region of the two subdomains, either force or energy is interpolated smoothly between the two distinct descriptions. Previous excellent technical reviews on this research line are also available (Praprotnik et al. 2008; Delle Site and Praprotnik 2017). Another interesting hybrid approach has been proposed recently in Scukins et al. (2015), where the hybrid MD/continuum hydrodynamics system of liquid water is considered as two completely miscible liquids using two-phase modeling, where one phase corresponding to the MD and the other to fluctuating continuum hydrodynamics.

For modeling biological functions and diseases, especially those being localized such as the endothelial glycocalyx layer (Weinbaum et al. 2007; Deng et al. 2012) and blood clot formation (Fogelson and Neeves 2015), the DDM appear to be very promising because one can treat different subdomains of the system using different models and methods. In this chapter, we discuss some of the important extensions of the DDM in the fields of multiscale modeling for simple and complex fluids. In the following, we shall first describe the DDM for simple fluids, which include some introduction materials on MD and NS equations. Furthermore, in the same section, we illustrate a few effective algorithms to couple the MD and NS descriptions, with a focus on constraining the artificial boundary of MD. Subsequently, we revisit the concepts of DDM for complex fluids or AdResS. Along the discussions of fundamental algorithms, we illustrate a few selected applications. We summarize this chapter in the end with some perspectives.

2 Domain Decomposition Methods for Simple Fluids

2.1 Molecular Dynamics

We consider a system of N identical, spherical, and structureless particles; they have the same mass m and are enclosed in a volume $\mathscr{V}$. The Hamiltonian $\mathscr{H}$ of the system is defined as

$$\mathscr{H}(\mathbf{r}^N, \mathbf{p}^N) = \sum_{i=1}^{N} \left[\frac{|\mathbf{p}_i|^2}{2m} + u_i(\mathbf{r}^N) \right], \tag{1}$$

where the first and second terms on the right-hand side are the kinetic and potential energies, respectively. The value of $(\mathbf{r}^N, \mathbf{p}^N)$ defines a phase point, where $\mathbf{r}^N = (\mathbf{r}_1, \mathbf{r}_2, \ldots, \mathbf{r}_N)$ are $3N$-dimensional coordinates and $\mathbf{p}^N = (\mathbf{p}_1, \mathbf{p}_2, \ldots, \mathbf{p}_N)$ are $3N$-dimensional momenta. In addition, velocity is defined as $\mathbf{v}_i = \mathbf{p}_i/m$. The trajectory of a phase point is determined by Hamilton's equations:

$$\dot{\mathbf{r}}_i = \frac{\partial \mathscr{H}}{\partial \mathbf{p}_i}, \quad \dot{\mathbf{p}}_i = -\frac{\partial \mathscr{H}}{\partial \mathbf{r}_i}. \tag{2}$$

More specifically, we consider an argon-like liquid described by a shifted Lennard-Jones (LJ) potential truncated at $r_{ij} = r_c$

$$u(r) = \begin{cases} 4\varepsilon \left[\left(\frac{\sigma}{r}\right)^{12} - \left(\frac{\sigma}{r}\right)^{6} - \left(\frac{\sigma}{r_c}\right)^{12} + \left(\frac{\sigma}{r_c}\right)^{6} \right], & r \le r_c \\ 0, & r > r_c \end{cases} \tag{3}$$

where ε and σ set the characteristic energy and length scales, respectively. Relative distance between particles is $r_{ij} = |\mathbf{r}_{ij}|$ and $\mathbf{e}_{ij} = \mathbf{r}_{ij}/r_{ij}$. The potential is pairwise,

and therefore, the potential energy of particle i is $u_i(\mathbf{r}^N) = 1/2 \sum_j^{N_{\text{neigh}}} u(r_{ij})$, where N_{neigh} is the number of neighboring particles within a spherical region of radius r_c around particle i. Hence, a pairwise force between particles i and j reads

$$\mathbf{F}_{ij} = -\frac{\partial u(r_{ij})}{\partial r_{ij}} \mathbf{e}_{ij}. \tag{4}$$

The MD trajectories evolve by a time integrator, such as the Verlet velocity algorithm (Allen and Tildesley 1989; Tuckerman 2010) with time step δt.

2.2 Navier-Stokes Equations

We consider an isothermal description of the fluids, where the energy or entropy change of the fluids is ignored. We have the conservations of mass and momentum densities as (Landau and Lifshitz 1987)

$$\frac{\partial \rho}{\partial t} + \nabla \cdot (\rho \mathbf{V}) = 0, \tag{5}$$

$$\frac{\partial \rho \mathbf{V}}{\partial t} + \nabla \cdot \Pi = 0, \tag{6}$$

where ρ, $\mathbf{V}$, and Π are density, velocity, and stress fields, respectively. Here velocity is capitalized to differentiate with the MD particle's velocity $\mathbf{v}$. For a compressible Newtonian fluid, the stress reads

$$\Pi = \rho \mathbf{V}\mathbf{V} - p\mathbf{I} - \eta \left(\nabla \mathbf{V} + \nabla \mathbf{V}^T \right) + \mathbf{I} \left(\frac{2}{3}\eta - \zeta \right) \nabla \cdot \mathbf{V}, \tag{7}$$

with $\mathbf{I}$ being the identity tensor and η and ζ the dynamic and bulk viscosities, respectively. The equation of state $p = p(\rho)$ and viscosities are usually obtained from MD simulations in the context of DDM for multiscale modeling. For an incompressible fluid, the term $\nabla \cdot \mathbf{V} = 0$ is dropped.

The Navier-Stokes equations are typically solved by mesh-based methods, such as finite difference, finite volume, and finite element, or other Lagrangian mesh-free particle methods.

2.3 Concurrent Coupling Between Particle Dynamics and Continuum Description

For illustrative purpose, we consider a specific hybrid simulation between MD and NS equations solved by a finite difference method (FDM). To demonstrate the concept, we take an example of unidirectional flow such as the Couette flow and

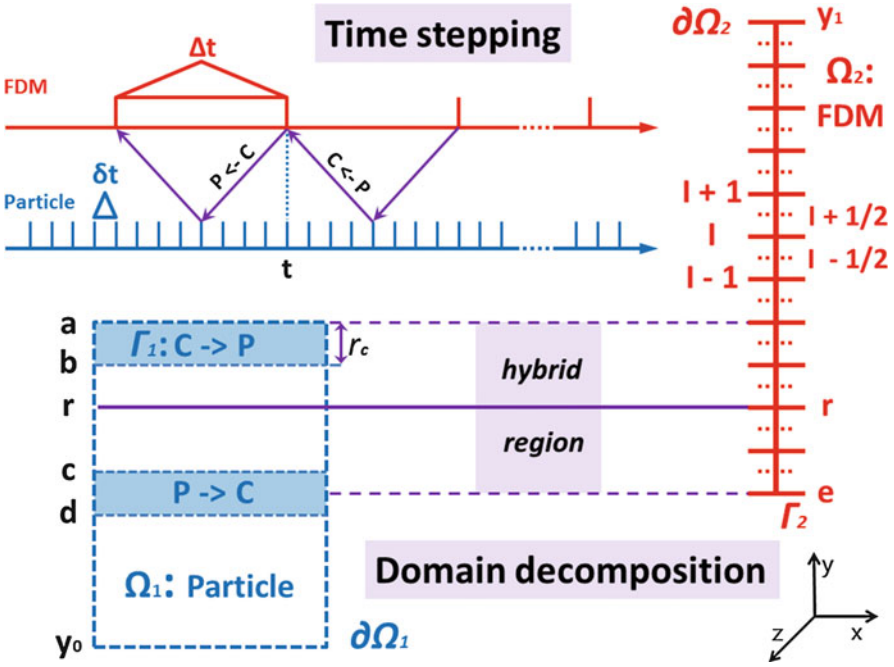

Fig. 1 (Color online) Sketch of a domain decomposition method and time stepping for coupling discrete particle dynamics with finite difference scheme. Subdomain Ω_1 is described by a molecular dynamics (MD) simulation, while subdomain Ω_2 is described by a finite difference method (FDM). The whole domain is bounded by two walls $\partial\Omega_1$ and $\partial\Omega_2$, at $y = y_0$ and y_1, respectively. An artificial boundary $\Gamma_1 : [y_b, y_a]$ applies to the MD, and an artificial boundary $\Gamma_2 : y = y_e$ applies to the FDM. A hybrid reference line is defined at $y = y_r$, at which the global solution is pieced together by combining results from MD below y_r and results from FDM above y_r. FDM runs with time step Δt, and DPD runs with time step δt, where $\Delta t = N_s \delta t$ and $N_s \gg 1$ is a positive integer. Time integrations of FDM and MD are staggered to synchronize. The communication time step between the two simulations is $\Delta t_{\text{comm}} = \Delta t$. The arrows between two time axes indicate information passing. (Modified from Bian et al. (2016))

couple the two descriptions along the y direction. This is best sketched in Fig. 1. The hybrid reference line is defined at y_r, and the global solution combines the solution of the MD below y_r and the solution of the FDM above y_r. The subdomain of MD is a three-dimensional box spanning $[0, L_{MD}] \times [0, L_{MD}]$ in x and z direction. In y direction, it ranges from $y_0 = 0$ to y_a. In the case of a wall-bounded domain, there are solid particles below y_0, and specific molecular interactions at fluid-solid interfaces that are different from fluid-fluid interactions must be taken into account. The FDM domain ranges from y_e to y_1 in y direction. No-slip or partial slip condition may apply at y_1 for the continuum description.

The time integrations of the two simulations are staggered to synchronize the average time progression. To minimize the lag time of information exchange (Bian et al. 2015b), we take communication time step $\Delta t_{\text{comm}} = \Delta t = N_s \delta t$. A typical

choice of N_s is an integer number so large ($N_s \gg 1$) that individual particle's velocity decorrelates after $N_s \delta t$ MD steps. This signifies the timescale separation of the two distinct descriptions of fluids; over each Δt the FDM follows a description of continuum mechanics, meanwhile the relevant molecular process reaches a quasi-stationary state. Therefore, given the intrinsic δt of MD and stability constraint on Δt, scale separation parameter N_s demands a low threshold for the grid size of FDM.

To couple the two scale descriptions, we have to pay more attention to the two artificial boundary regions Γ_1: $C \rightarrow P$ (continuum to particles) and Γ_2: $P \rightarrow C$ (particles to continuum). More specifically, on the communication between the two solvers, the particle simulation integrates with time step δt from $t = t - 3\Delta t/2$ to $t = t - \Delta t/2$. To impose the artificial boundary Γ_2 for the continuum ($P \rightarrow C$) at $t - \Delta t$, it is straightforward to perform simple spatial averaging on particle velocities between $y_d \leq y < y_c$ and thereafter temporal averaging over $t - 3\Delta t/2 < t \leq t - \Delta t/2$ as, for example, for the velocity state variable,

$$\mathbf{V}_e = \frac{1}{N_s} \sum_{j=1}^{N_s} \frac{1}{N_{cd}} \sum_{i=1}^{N_{cd}} \mathbf{v}_i. \tag{8}$$

Here, N_{cd} is the instantaneous number of particles located in cell $P \rightarrow C$. Furthermore, the region $P \rightarrow C$ is centered at $y = y_e$ with a thickness of r_c. Similarly, we may alternatively come up easily with the averaging procedures to impose mass and momentum fluxes at interface y_e of the FDM for compressible fluids as (Flekkøy et al. 2000)

$$\rho \mathbf{V} \cdot \mathbf{e}_y = \frac{1}{v_c} \sum_i m \mathbf{v}_i \cdot \mathbf{e}_y, \tag{9}$$

$$\Pi \cdot \mathbf{e}_y = \frac{1}{v_c} \sum_i \left(m \mathbf{v}_i \mathbf{v}_i + \frac{1}{2} \sum_{j \neq i} \mathbf{F}_{ij} \mathbf{r}_{ij} \right), \tag{10}$$

where $\mathbf{e}_y$ is the unit vector pointing outward at $y = y_e$ from FDM and v_c is the local cell volume centered at $y = y_e$ for spatial averaging. Furthermore, Eqs. (9) and (10) need temporal averaging over $t - 3\Delta t/2 < t \leq t - \Delta t/2$ as is done for Eq. (8). For non-isothermal case, energy flux can be imposed as well at the continuum interface (Delgado-Buscalioni and Coveney 2003a).

For more complex flow scenarios, a simple local-time-and-space averaging of particle quantities may not provide sufficiently smooth boundary conditions for the continuum description and may result in instability of the continuum solutions. Therefore, novel algorithms for noise reduction (Li et al. 1998; Grinberg 2012) are called for. Another alternative is to couple one continuum solver with multi-instance MD simulations, so the concept of ensemble averaging may be exploited (Neumann and Bian 2017).

Once $\mathbf{V}_e$ or the fluxes are updated at $t - \Delta t$, the FDM integrates one step from $t - \Delta t$ to t. Its new state variable solutions $\mathbf{V}_a$ and $\mathbf{V}_b$ at y_a and y_b or fluxes at y_a are passed to the particle simulation and are further utilized in various constraint dynamics (as explained in the next four subsections) to set the artificial boundary $\Gamma_1 : y_b \leq y < y_a$ of the particle simulation from $t - \Delta t/2$ to $t + \Delta t/2$. Meanwhile, the MD simulation integrates with time step δt from $t - \Delta t/2$ to $t + \Delta t/2$. Afterward, again Eq. (8) or Eqs. (9) and (10) are applied to impose state or flux boundary conditions of Γ_2 at t. The alternation of imposing artificial boundaries and the staggered integrations of the two simulations repeat until the end of the hybrid simulation.

Due to the truncation of the subdomain for the MD simulation, an average pressure force $\mathbf{F}^P(y)$ must be imposed at the truncation line $y = y_a$ inward. The best way to devise $\mathbf{F}^P(y)$ so far is to make use of the radial distribution function of particles and MD interacting forces to reflect the average effects outside y_a in the continuum limit. $\mathbf{F}^P$ is position-dependent and applies to each particle i within $y_a - y_i < r_c$ distance from y_a in the interior, that is, particles in Γ_1. This approach proves to induce negligible density oscillations near the artificial boundary (Werder et al. 2005; Lei et al. 2011). However, the imposed averaged force does not completely prevent particles from leaving outside. Therefore, a specular reflection or particle deletion is implemented at y_a. The former approach is more suitable to deal with an incompressible fluid, while the latter approach together with a particle insertion procedure (Delgado-Buscalioni and Coveney 2003b) is more physical to describe a compressible fluid by a grand-canonical ensemble so that the total number of particle in the MD subdomain fluctuates (Flekkøy et al. 2005).

The tricky part is to impose the artificial boundary in $\Gamma_1 (C \rightarrow P)$ for MD particles from $t - \Delta t/2$ to $t + \Delta t/2$. There is *no unique way* to achieve this, as many extra degrees of freedom on particles are under-determined. For coupling state variable, the usual strategy is to perform a constraint dynamics on each particle i in Γ_1 in such a way that

$$\frac{1}{N_{\Gamma_1}} \sum_{i=1}^{N_{\Gamma_1}} \mathbf{v}_i = \overline{\mathbf{V}}_{\Gamma_1}, \tag{11}$$

is satisfied at every δt or on average over $N_s \delta t$ and thermal fluctuations are affected as little as possible. Here, N_{Γ_1} is the instantaneous number of particles in Γ_1, and $\overline{\mathbf{V}}_{\Gamma_1}$ is the average velocity of the continuum solutions in the same region. In this case, $\overline{\mathbf{V}}_{\Gamma_1} = (\mathbf{V}_a + \mathbf{V}_b)/2$ at time t. For coupling the fluxes, it is similar that we need to spread fluxes (few degrees of freedom) obtained from the continuum solution to the particles within the artificial boundary Γ_1.

In the following, we shall focus on four popular algorithms of constraint dynamics in Γ_1. Since we deal primarily with a unidirectional flow for illustrative purpose, we use scalar variables instead of vector ones. The constraint of the particle dynamics is always performed in x direction of the flow, and therefore the index for x is omitted. Velocities in y and z directions are not altered by the constraint dynamics.

2.4 Relaxation Dynamics

A relaxation dynamics method was proposed in the first paper of hybrid simulations on liquid flow (O'Connell and Thompson 1995). Effectively it reads as

$$\dot{v}_i = \frac{F_i}{m} + \frac{\varepsilon}{\delta t}\left(\overline{V}_{\Gamma_1} - \frac{1}{N_{\Gamma_1}}\sum_{j=1}^{N_{\Gamma_1}} v_j\right), \tag{12}$$

where F_i is the usual total particle force on particle i. The rest of the terms on the right-hand side act as a relaxing force, which drives each particle i in Γ_1 toward the average velocity $\overline{V}_{\Gamma_1}$ over $\delta t/\varepsilon$ time period. In O'Connell and Thompson (1995), the continuum has the same time step as that of the particle simulation, that is, $\Delta t = \delta t$. Moreover, the relaxation parameter is chosen as $\varepsilon = 0.01$ for the particular properties of the fluid simulated, where the authors argue that a smaller value of ε provides inadequate coupling, while a larger value may lead to excessive damping of thermal fluctuations.

2.5 Maxwell Buffer

The Maxwell buffer was first proposed in Hadjiconstantinou and Patera (1997) as

$$v_i = V_i + \delta v_i, \tag{13}$$

$$V_i = V_b + (V_a - V_b)(y_i - y_b)/\Delta y, \tag{14}$$

where a deterministic component V_i is obtained by a linear interpolation between the values on the two nearest grid points V_a and V_b. Under the assumption of a local equilibrium for MD, the stochastic component δv_i is drawn from the Maxwell-Boltzmann distribution at a given temperature $k_B T$,

$$p(\delta v_i) = \sqrt{\frac{m}{2\pi k_B T}} \exp\left[\frac{-m(\delta v_i)^2}{2k_B T}\right]. \tag{15}$$

It is simple to see that Eqs. (13) and (14) satisfy directly the constraint posed in Eq. (11).

2.6 Least Constraint Dynamics

By taking the extremum of the time integral of the Lagrangian for the particles in Γ_1, which is subject to the non-holonomic constraint in Eq. (11), the equation of motion (EoM) for each particle i in Γ_1 is according to (Nie et al. 2004)

$$\dot{v}_i = \frac{F_i}{m} - \frac{1}{N_{\Gamma_1}} \sum_{j=1}^{N_{\Gamma_1}} \frac{F_j}{m} + \frac{1}{\delta t} \left(\overline{V}_{\Gamma_1} - \frac{1}{N_{\Gamma_1}} \sum_{j=1}^{N_{\Gamma_1}} v_j \right). \tag{16}$$

Instead of repeating the derivation for Eq. (16) as in Nie et al. (2004), we may arrive at the same expression from another perspective. To satisfy the constraint in Eq. (11), an extra body force $F^b_{\Gamma_1}$ is introduced *dynamically* at every time step δt such that (Werder et al. 2005)

$$\overline{v}'_{\Gamma_1} = \overline{v}_{\Gamma_1} + \frac{\delta t}{N_{\Gamma_1} m} (F_{\Gamma_1} + F^b_{\Gamma_1}), \tag{17}$$

where $\overline{v}_{\Gamma_1}$ is the average velocity and F_{Γ_1} is the total force in Γ_1 due to particle interactions,

$$\overline{v}_{\Gamma_1} = \frac{1}{N_{\Gamma_1}} \sum_{j=1}^{N_{\Gamma_1}} v_j, \quad F_{\Gamma_1} = \sum_{i=1}^{N_{\Gamma_1}} F_j. \tag{18}$$

To satisfy Eq. (11), we set $\overline{v}'_{\Gamma_1} = \overline{V}_{\Gamma_1}$, and therefore, we obtain an expression for the body force $F^b_{\Gamma_1}$ as

$$F^b_{\Gamma_1} = \frac{N_{\Gamma_1} m}{\delta t} (\overline{V}_{\Gamma_1} - \overline{v}_{\Gamma_1}) - F_{\Gamma_1} = \frac{N_{\Gamma_1} m}{\delta t} \left(\overline{V}_{\Gamma_1} - \frac{1}{N_{\Gamma_1}} \sum_{j=1}^{N_{\Gamma_1}} v_j \right) - \sum_{j=1}^{N_{\Gamma_1}} F_j. \tag{19}$$

The value of $F^b_{\Gamma_1}$ is dynamic and may vary at every δt. If we spread the body force $F^b_{\Gamma_1}$ from Eq. (19) *evenly* on N_{Γ_1} particles in Γ_1, it gives exactly the same EoM as in Eq. (16) for each particle i.

2.7 Flux-Exchange Coupling

The exchange of flux for dense fluids was first proposed in Flekkøy et al. (2000) and extended in Delgado-Buscalioni and Coveney (2003a). Rather than constraining the state variables directly, as done in the previous three methods, this method imposes flux at the truncation line y_a of the subdomain of particle simulation. Therefore, the EoM of particles in Γ_1 reads

$$\dot{v}_i = \frac{F_i}{m} + F^x(y_i), \quad F^x(y_i) = \tau^{xy}_a A \lambda(y_i), \tag{20}$$

where $A = L_x \times L_z$ is the surface area of the truncation and τ^{xy}_a is the shear stress at y_a from the continuum. The distribution function $\lambda(y_i)$ of the shear force on each particle must be normalized

$$\lambda(y_i) = g(y_i) / \sum_{j=1}^{N_{\Gamma_1}} g(y_j), \tag{21}$$

where $g(y)$ is an arbitrary function so that $\lambda(y)$ diverges at $y = y_a$ and decays to zero as y approaches y_b from y_a.

If we assume that there is a locally linear shear flow within Γ_1, which is a reasonable assumption for many flow problems, then the distribution function $\lambda(y)$ may be defined better than an arbitrary one (Ren 2007). By assuming a locally linear shear flow, we can work out the continuum limit of the shear forces on line y_a from particles within Γ_1. By setting the shear force on y_a from particles equal to the continuum solution of FDM at y_a, we have an identity as follows:

$$A\tau_a^{xy} = \int_0^{r_c} Ad\gamma^D(h)h\dot{\gamma}dh, \tag{22}$$

where h is the distance of particle i from y_a ($h = y_a - y_i$) and $\dot{\gamma}$ is an arbitrary shear rate, while given the particle interaction potential, $\gamma^D(h)$ can be numerically evaluated (Bian et al. 2016). Equation (22) holds for an arbitrary shear rate $\dot{\gamma}$. Therefore, given a shear stress τ^{xy} from the continuum solution of FDM, the distribution of shear force on each particle i is independent of $\dot{\gamma}$ as

$$F^x(y_i) = B_0\tau_a^{xy}\gamma^D(h)h, \tag{23}$$

where B_0 is a normalization constant for the particular particle simulation parameters.

2.8 Some Comments on Different Coupling Strategies

In order to bridge the concepts of state and flux coupling, Walther et al. (2012) applied the gradient of velocities averaged from MD simulations to impose the flux boundary condition on the lattice Boltzmann continuum solver. For conservation and stability purposes, we may have also a mixture of coupling state variables and fluxes; we refer to Flekkøy et al. (2005), Ren (2007), Bian et al. (2015b, 2016) and references therein for further discussions.

On the accuracy of the coupling schemes, the quantity of interest has been often the *mean field* variables, such as velocity, density, and stresses, which are sufficient from the continuum perspective. There has not been a consensus as to which of the four methods is most effective, as all the methods introduce above are actually capable of generating accurate mean profiles. For practical convenience, the relaxation dynamics involves an empirical parameter ε, which requires more trial-and-tune simulations. Therefore, the least constraint dynamics is preferred over the relaxation dynamics. The Maxwell buffer and flux exchange have the same easiness as the least constraint dynamics.

However, if we take a microscopic perspective and take the continuum description as a bath to supplement the truncated particle simulation, we may evaluate more closely certain quantities of interest in the particle region. For example, by calculating the fluctuation correlations between field variables of MD, we may compare the performance of the coupling schemes mentioned above (Bian et al. 2015a, 2016, 2018). It turns out that we have two sources of errors in the particle region; one is due to the truncation of the particle domain, and the other is due to the constraint dynamics performed on the particles in the artificial boundary. The first source of error is universal for different coupling strategies, and it may be almost completely removed by implementing an appropriate particle removal and insertion algorithm to mimic the grand-canonical ensemble of the an open particle system (Delgado-Buscalioni and Coveney 2003b; Delle Site and Praprotnik 2017). On the second source of error, the Maxwell buffer completely ignores any intrinsic thermal velocity correlations between particles and simply constrains individual particle's velocity as identical independent Gaussian distribution in the artificial boundary, therefore introducing the most artifacts, whereas the other constraint algorithms are relatively mild and commit much smaller error on this aspect (Bian et al. 2016).

Furthermore, if the overlapping region between particle and continuum subdomain increases, that is, if we can afford to perform extra volume of particle simulation, the contaminations of all the constraint dynamics on the thermal fluctuation correlations have very similar behavior, and the negative effects decrease linearly as the size of the overlap increases (Bian et al. 2016).

Thus far, there has been quite a few applications which were enabled by the DDM for multiscale modeling, bridging the atomistic and continuum descriptions. One of the most apparent classes of application is to model local or singular effects accurately with MD and capture bulk macroscopic flow behavior elsewhere with NS equations. This type of problem includes the fluid-solid boundary conditions with flow slip or epitaxial growth taking place (Thompson and Robbins 1990; O'Connell and Thompson 1995), contact line problem with contact angle as a dynamic variable (Hadjiconstantinou 1999), lid-driven cavity flow with singular stress at the corner (Nie et al. 2006), sound propagation through lipid monolayer (De Fabritiis et al. 2006), platelet deposition on the wall of a brain aneurysm (Grinberg et al. 2013), and so on. In the next section, however, we will describe a triple-scale approach that couples atomistic and continuum hydrodynamics through an intermediate CG description.

3 Domain Decomposition Methods for Complex Fluids: Adaptive Resolution Scheme

Another branch of DDM is related to coupling fine and CG descriptions of soft matter and molecular liquids within a particle-based framework. Similarly to other domain decomposition approaches, the aim of such adaptive resolution simulations is to model the interesting part of the system with the detailed atomistic (AT)

resolution, which is coupled with a CG representation of the remaining part of the system. Among the most advanced multiscale methods for conducting this kind of molecular simulations is the adaptive resolution scheme (AdResS) (Praprotnik et al. 2005, 2008, 2011). The method can successfully couple two or more levels of resolution concurrently present in the system. AdResS enables the particles to change their resolution on the fly, during the course of an MD simulation. The method is suitable for molecular systems where the AT resolution is required only in a spatially localized region, whereas a lower CG level of detail is sufficient for the rest of the system. Such cases are typically found in simulations of biological macromolecules, e.g., DNA. There, the AT resolution is required only for the macromolecule and the solvent in its vicinity, whereas the solvent farther away is adequately treated on a simplified CG level.

AdResS allows molecules to freely move across different regions and change their resolution on the fly according to their position in the system. When a CG molecule leaves the CG domain, it is remapped into the atomistically resolved molecule with a random orientation. To avoid any overlaps of its atoms with the atoms of the neighboring molecules, it is required that introduction of the atomistic degrees of freedom is continuous and not instantaneous. To this end, an interface layer between the AT and CG regions is introduced that allows an atomistic molecule to gradually find an energetically permissible orientation with respect to its neighboring molecules. This transition region, also called a hybrid (HY) region, contains hybrid molecules where both representations are superimposed.

Two levels of resolution are coupled via a force interpolation scheme. The intermolecular force between given molecules α and β is defined as

$$\mathbf{F}_{\alpha\beta}^{\mathrm{AdResS}} = w(X_\alpha)w(X_\beta)\mathbf{F}_{\alpha\beta}^{AT} + [1 - w(X_\alpha)w(X_\beta)]\mathbf{F}_{\alpha\beta}^{CG}, \tag{24}$$

where X_α and X_β are the centers-of-mass positions of the molecules α and β, respectively, and w is a weighting function that governs the transition between different resolution regions and therefore needs to be smooth. This function depends on the position of the mapping point of the molecule and is defined in the following way: $w = 1$ corresponds to the AT region and $w = 0$ to the CG region, whereas the values $0 < w < 1$ correspond to the HY region.

Original variant of the AdResS based on the force coupling above does not allow for a definition of a Hamiltonian and consequently has to be employed in conjunction with a thermostat. A recent Hamiltonian version of the method, i.e., H-AdResS (Potestio et al. 2013b; Everaers, R. 2016; Español et al. 2015), on the other hand, allows for the definition of a global Hamiltonian. This enables one to perform adaptive resolution Monte Carlo simulations (Potestio et al. 2013a). However, as the translation invariance is broken due to the resolution change, this implies that the total linear momentum cannot be conserved by H-AdResS. Since the linear momentum conservation is crucial for hydrodynamics, the original AdResS, which is not Hamiltonian, can therefore preserve linear momentum despite broken translational symmetry and is thus more convenient for coupling with the continuum hydrodynamics, as described below. Recent extensions of AdResS

also involve coupling to a quantum level of description (Poma and Delle Site 2010, 2011; Agarwal and Delle Site 2015, 2016; Delle Site 2018) as well as to open systems that exchange mass, momentum, and energy with their surroundings (Delgado-Buscalioni et al. 2015; Sablić et al. 2016; Wang et al. 2013; Agarwal et al. 2014, 2015; Delle Site 2016; Mukherji and Kremer 2013; Kreis et al. 2015). This allows for conducting MD simulations either in the grand-canonical statistical ensemble or under non-equilibrium conditions (Delgado-Buscalioni et al. 2015; Sablić et al. 2016, 2017b; Delle Site 2018). AdResS has been successfully applied to biomolecular systems (Zavadlav et al. 2017) such as proteins (Zavadlav et al. 2014; Fogarty et al. 2015) and DNA molecules (Zavadlav et al. 2015a,b, 2016b) solvated in multiscale solvents (Bevc et al. 2013; Nagarajan et al. 2013; Zavadlav et al. 2014, 2015b). In connection to hydrodynamics phenomena, AdResS has also been used to couple MD to the dissipative particle dynamics (DPD) method (Hoogerbrugge and Koelman 1992; Español and Warren 1995, 2017; Groot and Warren 1997; Español 1995), the multiparticle collision dynamics (MPC) (Malevanets and Kapral 1999), and smoothed dissipative particle dynamics (SDPD) (Español and Revenga 2003; Vázquez-Quesada et al. 2009). In the DPD, groups of atoms/molecules are lumped to form soft beads that interact via explicit soft conservative, random, and dissipative forces to simulate fluids on a mesoscopic scale with correct hydrodynamics interactions. In the SDPD, the Navier-Stokes equations are numerically solved with a formalism that is reminiscent of MD, whereas in the MPC the system is modeled by particles with continuous positions and velocities and stochastic interparticle interactions. Thus, using AdResS Petsev et al. (2015, 2017) coupled the MD to SDPD, whereas Alekseeva et al. (2016) linked the MD with MPC. The robustness of both hybrid approaches was demonstrated on a Lennard-Jones fluid. AdResS has been also applied to couple MD with DPD water (Zavadlav and Praprotnik 2017). In this chapter, however, we will focus on coupling with the continuum hydrodynamics (Delgado-Buscalioni et al. 2008, 2009, 2015).

One can combine AdResS with the flux-exchange coupling (Flekkøy et al. 2000; Delgado-Buscalioni and Coveney 2003a, 2004; Delgado-Buscalioni et al. 2005; Flekkøy et al. 2005; De Fabritiis et al. 2006; Delgado-Buscalioni and De Fabritiis 2007), described in Sect. 2.7, to link an MD with a continuum hydrodynamic domain, resulting in a triple-scale setup (Delgado-Buscalioni et al. 2008, 2009), as depicted in Fig. 2. In this triple-scale approach, the particle-based domain is simulated by MD simulation. The dynamics of molecules is thus governed by Newton's equations of motion, as explained in Sect. 2.1. On the other hand, continuum description enables the study of macroscopic fluid flows. The fluid is described by Navier-Stokes equations (see Sect. 2.2). The Navier-Stokes equations can be numerically solved in different ways (Koumoutsakos 2005), e.g., the finite volume method, where the continuum region is divided into small cells of volume (De Fabritiis et al. 2006; Delgado-Buscalioni et al. 2008). In such a way, discretized Navier-Stokes equations are then integrated in time using an explicit Euler scheme (Delgado-Buscalioni and De Fabritiis 2007).

The MD and continuum domains share an interface, as shown in Fig. 2. The otherwise independent MD and continuum domains exchange information after

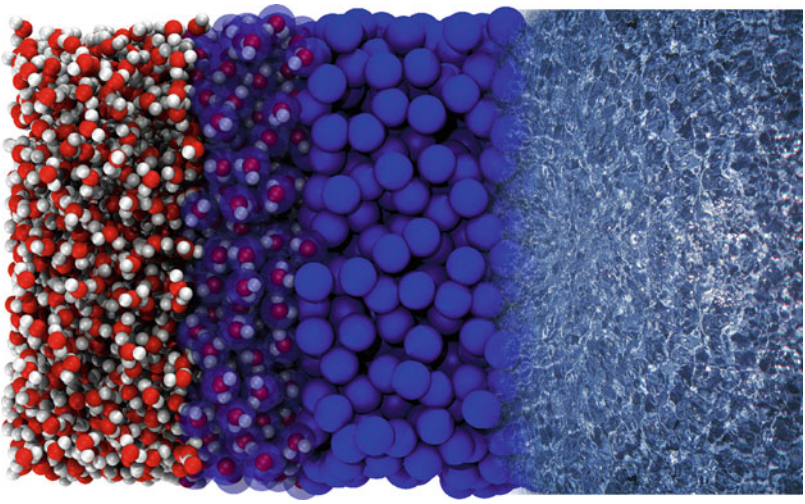

Fig. 2 Domain decomposition of triple-scale liquid water system: coupling of atomistic and continuum hydrodynamics. The MD domain contains atomistic and coarse-grained water molecules, whereas the continuum domain is solved by computational fluid dynamics approach. (Reprinted from Delgado-Buscalioni et al. 2015)

every fixed time interval Δt (Delgado-Buscalioni et al. 2008). Flux balance implies the conservation of mass and momentum across the interface, i.e., both domains should receive equally large but oppositely signed mass and momentum transfer across the interface over each Δt. The momentum flux across the interface is then used to update the flow variables at the continuum boundary cells. In turn, the same (but oppositely signed) flux needs to be imposed into the particle system across the interface (see Sect. 2.3).

The triple-scale method has been applied to simple liquids, i.e., liquid of tetrahedral molecules and water (Delgado-Buscalioni et al. 2008, 2009). Equilibrium structural properties, i.e., the radial distribution function and density profile, in MD domain of the triple-scale system have been validated against reference all-atom MD simulations. Furthermore, the mass fluctuations of the open MD domain were demonstrated to agree with the theoretical grand-canonical predictions (Delgado-Buscalioni et al. 2009). The fluids were also exposed to the Couette and Stokes flows (Delgado-Buscalioni et al. 2008, 2009), and the resulting velocity profiles agreed with continuum hydrodynamics.

Of course, the underlying idea of this triple-scale scheme is that AdResS plays the role of the inserting facility for complex molecules such as star polymers (Delgado-Buscalioni et al. 2015; Sablić et al. 2016, 2017a,b). In the CG domain, a given star polymer, consisting of several tens of monomers, is represented with only one very soft CG bead. We face the problem of inserting new molecules into a dense liquid. Thus, the idea behind the resolution change is that AdResS allows the insertion of molecules of arbitrary size into the system. The CG domains act as

a mass reservoir where large molecules can be easily inserted due to soft effective interactions among CG beads (Delgado-Buscalioni and Coveney 2003a; De Fabritiis et al. 2004; Borg et al. 2014). Then, as the molecules move toward the AT domain, they gain the fine-grained details employing AdResS.

4 Summary and Perspectives

We have presented the DDM for multiscale modeling of simple and complex fluids. For simple fluids we employ a perspective of continuum mechanics, where state field variables and fluxes are fundamental quantities. Therefore, it is natural to couple state variables and/or fluxes between a particle simulation (e.g., MD) simulation with a NS solver. Within this perspective, the MD resolves local effects and provides macroscopic averages as a closure for the NS equations. Other physical quantities in MD that are not needed for NS are considered as unwanted, ignored, or filtered out. Consequently, various constraint dynamics on state variable or fluxes of MD are all effective and do not have apparent difference on the hybrid coupled simulations. If we are interested not only in the macroscopic behavior but also in certain mesoscopic or microscopic physics of the particle simulation in the course of hybrid simulation, the conclusion is different. For example, thermal fluctuations are hallmarks, and one of the driving mechanisms for physical processes at micro-/mesoscopic scales. If we evaluate the correlations of the thermal fluctuations in the particle simulations in the context of a hybrid simulation, we find that the constraint algorithm of Maxwell buffer ignores the local correlations completely, while other three constraint dynamics are relatively better at preserving the natural properties of the particle simulations.

We have also briefly presented the particle-based multiscale linear-momentum-preserving AdResS for coupling fine and CG molecular representations. AdResS is suitable to simulate fluids on the micro-/mesoscopic scale, where hydrodynamics plays an important role. In this spirit, AdResS has been recently applied to link MD and DPD methods for simulation of water at ambient conditions (Zavadlav and Praprotnik 2017). As the DPD water model corresponds to several water molecules, the supramolecular coupling is enabled by a recently developed clustering algorithm SWINGER that assembles, disassembles, and reassembles clusters as needed during the course of the simulation (Zavadlav et al. 2016a). This allows for a seamless coupling between standard atomistic MD and DPD models. In the future, this framework could be applied to important problems such as abnormal rheological and biomechanical properties of red blood cells encountered in disease states (Chang et al. 2016; Altenhoff et al. 2007; Rossinelli et al. 2015; Fedosov et al. 2010, 2011).

In this chapter, we focus on the DDM for fluids, and for readers interested in DDM for solid materials, there are quite a few excellent technical reviews, e.g., Miller and Tadmor (2009). There are other multiscale modeling methods tightly related to DDM, such as *CONFFESSIT* (Laso and Öttinger 1993) and *heterogeneous multiscale method* (Ren and Weinan 2005; Weinan et al. 2007; Borg et al. 2013; Yasuda and Yamamoto 2010), where a macroscopic model is selected for

the whole domain and a microscopic solver is utilized to provide fine details such as boundary conditions or constitutive relations wherever needed. Along the research line of adaptive mesh refinement, Garcia et al. also develop the algorithm refinement technique at the finest scale of the mesh to switch on microscopic description such as the direction simulation of Monte Carlo (Garcia et al. 1999). Kevrekidis and colleagues propose space-selective microscopic descriptions without a macroscopic equation (therefore, named as *equation-free*) (Kevrekidis and Samaey 2009). By employing novel gap-tooth interpolation in space and projection in time, the equation-free framework is able to perform system-level tasks and predictions.

There are also a few high-performance software packages free for usage (Tang et al. 2015; Neumann and Bian 2017; Halverson et al. 2013). Together with the algorithm developments, they will foster further applications of DDM for multiscale modeling.

Acknowledgments Xin Bian acknowledges Prof. George Em Karniadakis, who led him to the research field of DDM for multiscale modeling. During his postdoctoral period, Xin benefited enormously from discussions with Prof. Karniadakis and his group. Xin Bian is also grateful for the discussions and full support from Prof. Nikolaus A. Adams, without whom the completeness of this work is impossible. Matej Praprotnik would like to thank Rafael Delgado-Buscalioni, Kurt Kremer, Luigi Delle Site, Jens H. Walther, and Petros Koumoutsakos for discussions and collaboration on this topic. He also acknowledges financial support from the Slovenian Research Agency (research core funding No. P1-0002 and the project J1-7435).

References

Agarwal A, Delle Site L (2015) Path integral molecular dynamics within the grand canonical-like adaptive resolution technique: simulation of liquid water. J Chem Phys 143:094102

Agarwal A, Delle Site L (2016) Grand-canonical adaptive resolution centroid molecular dynamics: implementation and application. Comput Phys Commun 206:26

Agarwal A, Wang H, Schütte C, Delle Site L (2014) Chemical potential of liquids and mixtures via adaptive resolution simulation. J Chem Phys 141:034102

Agarwal A, Zhu J, Hartmann C, Wang H, Delle Site L (2015) Molecular dynamics in a grand ensemble: Bergmann-Lebowitz model and adaptive resolution simulation. New J Phys 17:083042

Alekseeva U, Winkler RG, Sutmann G (2016) Hydrodynamics in adaptive resolution particle simulations: multiparticle collision dynamics. J Comput Phys 314:14–34

Allen MP, Tildesley DJ (1989) Computer simulation of liquids. Clarendon Press, Oxford

Altenhoff AM, Walther JH, Koumoutsakos P (2007) A stochastic boundary forcing for dissipative particle dynamics. J Comp Phys 225:1125–1136

Bevc S, Junghans C, Kremer K, Praprotnik M (2013) Adaptive resolution simulation of salt solutions. New J Phys 15:105007

Bian X, Li Z, Deng M, Karniadakis GE (2015a) Fluctuating hydrodynamics in periodic domains and heterogeneous adjacent multidomains: thermal equilibrium. Phys Rev E 92:053302

Bian X, Li Z, Karniadakis GE (2015b) Multi-resolution flow simulations by smoothed particle hydrodynamics via domain decomposition. J Comput Phys 297:132–155

Bian X, Deng M, Tang YH, Karniadakis GE (2016) Analysis of hydrodynamic fluctuations in heterogeneous adjacent multidomains in shear flow. Phys Rev E 93:033312

Bian X, Deng M, Karniadakis GE (2018) Analytical and computational studies of correlations of hydrodynamic fluctuations in shear flow. Commun Comput Phys 23:93–117

Borg MK, Lockerby DA, Reese JM (2013) A multiscale method for micro/nano flows of high aspect ratio. J Comput Phys 233:400–413
Borg MK, Lockerby DA, Reese JM (2014) The fade mass-stat: a technique for inserting or deleting particles in molecular dynamics simulations. J Chem Phys 140(7):074110
Chang H, Li X, Li H, Karniadakis GE (2016) Md/dpd multiscale framework for predicting morphology and stresses of red blood cells in health and disease. PLOS Comput Bio 12:e1005173
De Fabritiis G, Delgado-Buscalioni R, Coveney PV (2004) Energy controlled insertion of polar molecules in dense fluids. J Chem Phys 121(24):12139–12142
De Fabritiis G, Delgado-Buscalioni R, Coveney PV (2006) Multiscale modeling of liquids with molecular specificity. Phys Rev Lett 97:134501
Delgado-Buscalioni R (2012) Tools for multiscale simulation of liquids using open molecular dynamics. In: Engquist B, Runborg O, Tsai YHR (eds) Numerical analysis of multiscale computations, vol 82. Springer, Berlin/Heidelberg, pp 145–166
Delgado-Buscalioni R, Coveney PV (2003a) Continuum-particle hybrid coupling for mass, momentum, and energy transfers in unsteady fluid flow. Phys Rev E 67:046704
Delgado-Buscalioni R, Coveney PV (2003b) USHER: an algorithm for particle insertion in dense fluids. J Chem Phys 119:978–987
Delgado-Buscalioni R, Coveney P (2004) Hybrid molecularcontinuum fluid dynamics. Phil Trans R Soc A 362(1821):1639–1654
Delgado-Buscalioni R, De Fabritiis G (2007) Embedding molecular dynamics within fluctuating hydrodynamics in multiscale simulations of liquids. Phys Rev E 76:036709
Delgado-Buscalioni R, Flekkøy EG, Coveney PV (2005) Fluctuations and continuity in particle-continuum hybrid simulations of unsteady flows based on flux-exchange. EPL 69(6):959
Delgado-Buscalioni R, Kremer K, Praprotnik M (2008) Concurrent triple-scale simulation of molecular liquids. J Chem Phys 128:114110
Delgado-Buscalioni R, Kremer K, Praprotnik M (2009) Coupling atomistic and continuum hydrodynamics through a mesoscopic model: application to liquid water. J Chem Phys 131:244107
Delgado-Buscalioni R, Sablić J, Praprotnik M (2015) Open boundary molecular dynamics. Eur Phys J Special Top 224:2331–2349
Delle Site L (2016) Formulation of Liouville's theorem for grand ensemble molecular simulations. Phys Rev E 93:022130
Delle Site L (2018) Grand canonical adaptive resolution simulation for molecules with electrons: a theoretical framework based on physical consistency. Comput Phys Commun 222:94–101
Delle Site L, Praprotnik M (2017) Molecular systems with open boundaries: theory and simulation. Phys Rep 693:1–56
Deng M, Li X, Liang H, Caswell B, Karniadakis GE (2012) Simulation and modeling of slip flow over surfaces grafted with polymer brushes and glycocalyx fibres. J Fluid Mech 711:192–211
Español P (1995) Hydrodynamics from dissipative particle dynamics. Phys Rev E 52(2):1734–1742
Español P, Revenga M (2003) Smoothed dissipative particle dynamics. Phys Rev E 67(2):026705
Español P, Warren P (1995) Statistical mechanics of dissipative particle dynamics. Europhys Lett 30(4):191–196
Español P, Warren PB (2017) Perspective: dissipative particle dynamics. J Chem Phys 146(15):150901
Español P, Delgado-Buscalioni R, Everaers R, Potestio R, Donadio D, Kremer K (2015) Statistical mechanics of hamiltonian adaptive resolution simulations. J Chem Phys 142:064115
Everaers, R (2016) Thermodynamic translational invariance in concurrent multiscale simulations of liquids. Eur Phys J Special Top 225:1483–1503
Fedosov DA, Karniadakis GE (2009) Triple-decker: interfacing atomistic-mesoscopic-continuum flow regimes. J Comput Phys 228:1157–1171
Fedosov DA, Caswell B, Karniadakis GE (2010) A multiscale red blood cell model with accurate mechanics, rheology, and dynamics. Biophys J 98:2215–2225
Fedosov DA, Pan W, Caswell B, Gompper G, Karniadakis GE (2011) Predicting human blood viscosity in silico. Proc Natl Acad Sci USA 108:11772–11777

Flekkøy EG, Wagner G, Feder J (2000) Hybrid model for combined particle and continuum dynamics. Europhys Lett 52(3):271–276
Flekkøy EG, Delgado-Buscalioni R, Coveney PV (2005) Flux boundary conditions in particle simulations. Phys Rev E 72:026703
Fogarty AC, Potestio R, Kremer K (2015) Adaptive resolution simulation of a biomolecule and its hydration shell: structural and dynamical properties. J Chem Phys 142:195101
Fogelson AL, Neeves KB (2015) Fluid mechanics of blood clot formation. Ann Rev Fluid Mech 47(1):377–403
Garcia AL, Bell JB, Crutchfield WY, Alder BJ (1999) Adaptive mesh and algorithm refinement using direct simulation Monte Carlo. J Comput Phys 154(1):134–155
Grinberg L (2012) Proper orthogonal decomposition of atomistic flow simulations. J Comput Phys 231(16):5542–5556
Grinberg L, Fedosov DA, Karniadakis GE (2013) Parallel multiscale simulations of a brain aneurysm. J Comput Phys 244:131–147
Groot RD, Warren PB (1997) Dissipative particle dynamics: bridging the gap between atomistic and mesoscopic simulation. J Chem Phys 107(11):4423–4435
Hadjiconstantinou NG (1999) Hybrid atomisticcontinuum formulations and the moving contact-line problem. J Comput Phys 154(2):245–265
Hadjiconstantinou NG, Patera AT (1997) Heterogeneous atomistic-continuum representations for dense fluid systems. Int J Mod Phys C 08(04):967–976
Halverson JD, Brandes T, Lenz O, Arnold A, Bevc S, Starchenko V, Kremer K, Stuehn T, Reith D (2013) Espresso++: a modern multiscale simulation package for soft matter systems. Comput Phys Commun 184(4):1129–1149
Hoogerbrugge PJ, Koelman JMVA (1992) Simulating microsopic hydrodynamics phenomena with dissipative particle dynamics. Europhys Lett 19(3):155–160
Kevrekidis IG, Samaey G (2009) Equation-free multiscale computation: algorithms and applications. Annu Rev Phys Chem 60(1):321–344
Koumoutsakos P (2005) Multiscale flow simulations using particles. Ann Rev Fluid Mech 37:457–487
Kreis K, Fogarty A, Kremer K, Potestio R (2015) Advantages and challenges in coupling an ideal gas to atomistic models in adaptive resolution simulations. Eur Phys J Special Top 224:2289–2304
Landau LD, Lifshitz EM (1987) Fluid mechanics. Course of theoretical physics, vol 6, 2nd edn. Pergamon Press, Oxford
Laso M, Öttinger HC (1993) Calculation of viscoelastic flow using molecular models: the CONNFFESSIT approach. J Non-Newton Fluid Mech 47:1–20
Lei H, Fedosov DA, Karniadakis GE (2011) Time-dependent and outflow boundary conditions for dissipative particle dynamics. J Comput Phys 230:3765–3779
Li J, Liao D, Yip S (1998) Coupling continuum to molecular-dynamics simulation: reflecting particle method and the field estimator. Phys Rev E 57:7259–7267
Malevanets A, Kapral R (1999) Mesoscopic model for solvent dynamics. J Chem Phys 110(17):8605–8613
Miller RE, Tadmor EB (2009) A unified framework and performance benchmark of fourteen multiscale atomistic/continuum coupling methods. Model Simul Mater Sci Eng 17(5): 053001
Mohamed K, Mohamad A (2010) A review of the development of hybrid atomistic-continuum methods for dense fluids. Microfluid Nanofluid 8(3):283–302
Mukherji D, Kremer K (2013) Coil-globule-coil transition of PNIPAm in aqueous methanol: coupling all-atom simulations to semi-grand canonical coarse-grained reservoir. Macromolecules 46(22):9158–9163
Nagarajan A, Junghans C, Matysiak S (2013) Multiscale simulation of liquid water using a four-to-one mapping for coarse-graining. J Chem Theory Comput 9:5168–5175
Neumann P, Bian X (2017) MaMiCo: transient multi-instance molecular-continuum flow simulation on super-computers. Comput Phys Commun 220:390–402

Nie XB, Chen SY, Weinan E, Robbins MO (2004) A continuum and molecular dynamics hybrid method for micro- and nano-fluid flow. J Fluid Mech 500:55–64
Nie X, Robbins MO, Chen S (2006) Resolving singular forces in cavity flow: multiscale modeling from atomic to millimeter scales. Phys Rev Lett 96:134501
O'Connell ST, Thompson PA (1995) Molecular dynamics-continuum hybrid computations: a tool for studying complex fluid flows. Phys Rev E 52:R5792–R5795
Petsev ND, Leal LG, Shell MS (2015) Hybrid molecular-continuum simulations using smoothed dissipative particle dynamics. J Chem Phys 142(4):044101
Petsev ND, Leal LG, Shell MS (2017) Coupling discrete and continuum concentration particle models for multiscale and hybrid molecular-continuum simulations. J Chem Phys 147:234112
Pivkin IV, Karniadakis GE (2006) Controlling density fluctuations in wall-bounded dissipative particle dynamics systems. Phys Rev Lett 96:206001
Poma A, Delle Site L (2010) Classical to path-integral adaptive resolution in molecular simulation: towards a smooth quantum-classical coupling. Phys Rev Lett 104:250201
Poma A, Delle Site L (2011) Adaptive resolution simulation of liquid para-hydrogen: testing the robustness of the quantum-classical adaptive coupling. Phys Chem Chem Phys 13: 10510
Potestio R, Español P, Delgado-Buscalioni R, Everaers R, Kremer K, Donadio D (2013a) Monte Carlo adaptive resolution simulation of multicomponent molecular liquids. Phys Rev Lett 111:060601
Potestio R, Fritsch S, Español P, Delgado-Buscalioni R, Kremer K, Everaers R, Donadio D (2013b) Hamiltonian adaptive resolution simulation for molecular liquids. Phys Rev Lett 110:108301
Praprotnik M, Delle Site L, Kremer K (2005) Adaptive resolution molecular-dynamics simulation: changing the degrees of freedom on the fly. J Chem Phys 123(22):224106
Praprotnik M, Delle Site L, Kremer K (2008) Multiscale simulation of soft matter: from scale bridging to adaptive resolution. Annu Rev Phys Chem 59:545–571
Praprotnik M, Poblete S, Kremer K (2011) Statistical physics problems in adaptive resolution computer simulations of complex fluids. J Stat Phys 145:946–966
Quarteroni A, Valli A (1999) Domain decomposition methods for partial differential equations. Oxford science publications, Oxford
Ren W (2007) Analytical and numerical study of coupled atomistic-continuum methods for fluids. J Comput Phys 227(2):1353–1371
Ren W, Weinan EW (2005) Heterogeneous multiscale method for the modeling of complex fluids and micro-fluidics. J Comput Phys 204(1):1–26
Rossinelli D, Tang YH, Lykov K, Alexeev D, Bernaschi M, Hadjidoukas P, Bisson M, Joubert W, Conti C, Karniadakis G, Fatica M, Pivkin I, Koumoutsakos P (2015) The in-silico lab-on-a-chip: petascale and high-throughput simulations of microfluidics at cell resolution. In: Proceedings of the international conference for high performance computing, networking, storage and analysis, SC'15, vol 2, ACM, New York, pp 1–12
Sablić J, Praprotnik M, Delgado-Buscalioni R (2016) Open boundary molecular dynamics of sheared star-polymer melts. Soft Matter 12:2416–2439
Sablić J, Delgado-Buscalioni R, Praprotnik M (2017a) Application of the eckart frame to soft matter: rotation of star polymers under shear flow. Soft Matter 13:6988–7000
Sablić J, Praprotnik M, Delgado-Buscalioni R (2017b) Deciphering the dynamics of star molecules in shear flow. Soft Matter 13:4971–4987
Scukins A, Nerukh D, Pavlov E, Karabasov S, Markesteijn A (2015) Multiscale molecular dynamics/hydrodynamics implementation of two dimensional "mercedes benz" water model. Euro Phys J Special Top 224(12):2217–2238
Smith B, Bjørstad P, Gropp W (1996) Domain decomposition: parallel multilevel methods for elliptic partial differential equations. Cambridge University Press, New York
Tang YH, Kudo S, Bian X, Li Z, Karniadakis GE (2015) Multiscale universal interface: a concurrent framework for coupling heterogeneous solvers. J Comput Phys 297:13–31
Thompson PA, Robbins MO (1990) Shear flow near solids: epitaxial order and flow boundary conditions. Phys Rev A 41:6830–6837

Toselli A, Widlund OB (2005) Domain decomposition methods–algorithms and theory. Springer, Berlin/Heidelberg

Tuckerman ME (2010) Statistical mechanics: theory and molecular simulation. Oxford University Press, Oxford

Vázquez-Quesada A, Ellero M, Español P (2009) Consistent scaling of thermal fluctuations in smoothed dissipative particle dynamics. J Chem Phys 130(3):034901

Walther JH, Praprotnik M, Kotsalis EM, Koumoutsakos P (2012) Multiscale simulation of water flow past a C540 fullerene. J Comput Phys 231(7):2677–2681

Wang H, Hartmann C, Schütte C, Delle Site L (2013) Grand-canonical-like molecular-dynamics simulations by using an adaptive-resolution technique. Phys Rev X 3:011018

Warshel A, Karplus M (1972) Calculation of ground and excited state potential surfaces of conjugated molecules. I. Formulation and parametrization. J Am Chem Soc 94(16):5612–5625

Warshel A, Levitt M (1976) Theoretical studies of enzymic reactions: dielectric, electrostatic and steric stabilization of the carbonium ion in the reaction of lysozyme. J Mole Bio 103(2):227–249

Weinan EW, Engquist B, Li X, Ren W, Vanden-Eijnden E (2007) Heterogeneous multiscale method: a review. Commun Comput Phys 2(3):367–450

Weinbaum S, Tarbell JM, Damiano ER (2007) The structure and function of the endothelial glycocalyx layer. Ann Rev Biomed Eng 9(1):121–167

Werder T, Walther JH, Koumoutsakos P (2005) Hybrid atomistic-continuum method for the simulation of dense fluid flows. J Comput Phys 205:373–390

Wijesinghe HS, Hadjiconstantinou NG (2004) Discussion of hybrid atomistic-continuum methods for multiscale hydrodynamics. Inter J Multi Comput Eng 2(2):189–202

Yasuda S, Yamamoto R (2010) Multiscale modeling and simulation for polymer melt flows between parallel plates. Phys Rev E 81:036308

Zavadlav J, Praprotnik M (2017) Adaptive resolution simulations coupling atomistic water to dissipative particle dynamics. J Chem Phys 147:114110

Zavadlav J, Melo MN, Marrink SJ, Praprotnik M (2014) Adaptive resolution simulation of an atomistic protein in MARTINI water. J Chem Phys 140:054114

Zavadlav J, Melo MN, Marrink SJ, Praprotnik M (2015a) Adaptive resolution simulation of polarizable supramolecular coarse-grained water models. J Chem Phys 142:244118

Zavadlav J, Podgornik R, Praprotnik M (2015b) Adaptive resolution simulation of a DNA molecule in salt solution. J Chem Theory Comput 11:5035–5044

Zavadlav J, Marrink SJ, Praprotnik M (2016a) Adaptive resolution simulation of supramolecular water: the concurrent making, breaking, and remaking of water bundles. J Chem Theory Comput 12:4138–4145

Zavadlav J, Podgornik R, Melo MN, Marrink SJ, Praprotnik M (2016b) Adaptive resolution simulation of an atomistic DNA molecule in MARTINI salt solution. Eur Phys J Spec Top 225:1595–1607

Zavadlav J, Bevc S, Praprotnik M (2017) Adaptive resolution simulations of biomolecular systems. Eur Biophys J 46:821–835